

## Bachelor Thesis

### **Non-Intrusive Injection Control System for Alternative Fuel Conversions**

to attain the academic degree  
Bachelor of Engineering

submitted by:

**José Luiz Salles de Mendonça**

Matriculation number: 35756

<joseluiz.sallesdemendonca@hs-weingarten.de>

13<sup>th</sup> August, 2025

First Reviewer: Prof. Dr. André Kaufmann <andre.kaufmann@rwu.de>

Second Reviewer: Dipl.-Ing. Walter Schildhauer <schildhauer@speedwave.de>

## Declaration of Originality

With my signature I confirm that the submitted thesis

Non-Intrusive Injection Control System for Alternative Fuel Conversions

is original work and was written by me without further assistance. Appropriate credit has been given where reference has been made to the work of others.

The thesis was not examined before, nor has it been published. The submitted electronic version of the thesis matches the printed version.

**Addendum:** In the attachment "Documentation of the Use of AI Tools," I have outlined which AI tools I used, for what purpose they were used, and in what manner the usage occurred.

Weingarten, 13 Aug 2025

---

José Luiz S. Mendonça

# 1 Abstract

This thesis presents the development of a non-intrusive module that manipulates fuel injection in internal combustion engines while preserving Original Equipment Manufacturer (OEM) Engine Control Unit (ECU) functionality. The module intercepts and modifies injection pulses to adjust fuel quantity according to the requirements of alternative fuels.

The hardware design supports both low and high impedance injectors with a versatile peak-and-hold driver circuit, applicable to various engine configurations. Stoichiometric combustion calculations for several alternative fuels provided the theoretical foundation for the system's requirements.

Tests on a Weber 2-cylinder engine validated the module's capability to modify the air-fuel ratio in real time. Lambda sensor measurements confirmed successful manipulation of the fuel mixture, demonstrating the module's effectiveness at increasing injected fuel mass. Results indicate this approach enables adaptation of Internal Combustion Engine (ICE)s to alternative fuels without requiring extensive ECU modifications.

# Contents

<b>Declaration of Originality</b>	<b>2</b>
<b>1 Abstract</b>	<b>3</b>
<b>2 Introduction</b>	<b>11</b>
<b>3 Theoretical Background</b>	<b>13</b>
3.1 The Combustion of Alternative Fuels . . . . .	13
3.2 A Simple Model for Alternative Fuel Combustion . . . . .	14
3.2.1 Fuel and Air Properties . . . . .	14
3.2.2 Stoichiometric Requirements . . . . .	15
3.2.3 Exhaust Gas Composition . . . . .	15
3.2.4 Fuel Energy Calculation . . . . .	16
3.2.5 Engine Performance Calculations . . . . .	16
3.3 Fuel Injection Systems and Injection control . . . . .	16
3.4 Injector Driver Topologies . . . . .	18
<b>4 Preparation</b>	<b>21</b>
4.1 Injector Characterization . . . . .	22
<b>5 Prototype Design and Construction</b>	<b>26</b>
5.1 Technical Requirements . . . . .	26
5.2 System Architecture . . . . .	27
5.2.1 Input Block . . . . .	28
5.2.2 Power Management Block . . . . .	29
5.2.3 Control Block . . . . .	30
5.3 Output Block . . . . .	31
5.3.1 Current Control . . . . .	33

5.3.2 Kickback Protection . . . . .	34
5.4 Prototype Construction . . . . .	38
<b>6 Prototype Testing</b>	<b>40</b>
6.1 Testbench Testing . . . . .	40
6.1.1 Injector Driver Operation . . . . .	40
6.1.2 Logic Edge Case Testing . . . . .	41
6.2 Testing on the Weber motor . . . . .	42
<b>7 Conclusion</b>	<b>46</b>
7.1 Summary of Key Findings . . . . .	46
7.2 Accomplishment of Requirements . . . . .	46
7.3 Limitations and Challenges . . . . .	47
7.4 Outlook . . . . .	48
<b>References</b>	<b>50</b>
<b>Attachment: Documentation of the Use of AI Tools</b>	<b>52</b>

# List of Figures

1	Comparison of fuel mass demand per hub for different fuel types at varying engine loads . . . . .	17
2	Fuel Injection System Overview. Adapted from [7] . . . . .	17
3	Injector as an RL Circuit . . . . .	18
4	Comparison of Peak and Hold and Saturation Drivers. Adapted from [3] . . . . .	20
5	Test motor and measurement setup for injector characterization . . . . .	21
6	Injector Characterization: measured current (blue) vs simulated current (green) . .	23
7	Inductive Kickback from the Injector . . . . .	24
8	Block Diagram of the Prototype System . . . . .	27
9	Input Block Diagram . . . . .	28
10	Transient Voltage Suppressor (TVS) Diode protection on logic inputs and power terminals . . . . .	29
11	Control Logic Flowchart . . . . .	30
12	LM1949 Application Circuit. Adapted from [13] . . . . .	32
13	Freewheeling diode implementation for inductive kickback protection. The diode provides a path for the current to flow when the MOSFET switches off, limiting the voltage spike across the inductor. . . . .	35
14	Zener diode implementation for inductive kickback protection. The Zener diode clamps the voltage spike, protecting the MOSFET from high voltages. . . . .	36
15	Positive Feedback Paths when Driving Inductances. Adapted from [16] . . . . .	37
16	Simulation results with the added gate resistance: reduced ringing. . . . .	37
17	Complete System Block Diagram . . . . .	38
18	PCB Design for the Peak and Hold Injector Driver: (a) Back copper layer with short traces for high current paths, (b) Front copper layer with control circuitry, (c) 3D rendered view showing component placement (d), Enclosure with all components ready to be mounted on the motor . . . . .	39

19	Testbench setup for peak and hold driver testing . . . . .	40
20	Input Saturation pulse and Output Peak and Hold PWM signal . . . . .	41
21	Connection between module, ECU, and injectors . . . . .	42
22	Testing the prototype module on the Weber motor . . . . .	43

# Glossary

**AFR** Air-Fuel Ratio. 11, 13

**alternative fuel** Conventional fuels predominantly derive from petroleum sources. In contrast, alternative fuels fall into two main categories: biogenic and synthetic. Biogenic variants are produced from plant matter, agricultural residues, and organic waste materials including animal byproducts, collectively known as biofuels. Synthetic alternatives, however, are manufactured through chemical synthesis processes [1]. 3, 11

**atomization** The process of breaking down liquid fuel into fine droplets to ensure efficient mixing with air for combustion.. 31

**avalanche** A phenomenon in which a sudden increase in voltage across an inductor causes a rapid discharge of energy, often leading to high voltage spikes. This can occur when the current through an inductor is interrupted, and the energy stored in the magnetic field is released. 25

**deterministic** A system or process that behaves in a predictable manner, where the outcome is determined by initial conditions and parameters, without randomness or uncertainty. 31

**duty cycle** The ratio of the time a signal is active (high) to the total time of one cycle, expressed as a percentage. In the context of fuel injection, it refers to the proportion of time the fuel injector is open compared to the total time of the injection cycle. 22

**E-Fuel** synthetic fuels made by the use of electricity produced from water and CO<sub>2</sub> [2]. 11, 14

**ECU** Engine Control Unit. 3, 7, 11, 16, 18, 19, 21, 22, 24, 28, 29, 31, 33, 34, 42, 46

**EFI** Electronic Fuel Injection. 16, 18

**EOI** End of Injection. 27

**hydraulic lock** A condition in an internal combustion engine where a cylinder is filled with liquid fuel, preventing the piston from moving. This can occur if too much fuel is injected into the cylinder, leading to a situation where the piston cannot compress the liquid, potentially causing mechanical damage. 31

**hydrocarbon** A compound consisting primarily of hydrogen and carbon, commonly found in fossil fuels. 13

**ICE** Internal Combustion Engine. 3, 11

**injection pulse width** The duration of time for which the fuel injector is electrically activated and held open, controlling the amount of fuel delivered to the combustion chamber. It is measured in milliseconds and is directly proportional to the quantity of fuel injected. 18, 19, 22, 26, 28, 30, 31, 38

**MCU** Microcontroller Unit. 27, 28, 33, 38, 41

**OEM** Original Equipment Manufacturer. 3, 11, 34

**RL circuit** An electrical circuit consisting of a resistor (R) and an inductor (L). 18

**SOI** Start of Injection. 27

**stoichiometry** Stoichiometry is the calculation of reactants and products in a balanced chemical reaction . 13

**time constant** The time that it takes for the voltage or current to rise or fall to approximately 63.2% of its final value. 23

**TVS** Transient Voltage Suppressor. 6, 29, 33

**wasted spark** A type of ignition system where each spark plug fires twice per engine cycle, once during the compression stroke and once during the exhaust stroke, effectively "wasting" the spark on the exhaust stroke.. 22

**WCET** Worst Case Execution Time. 42

## 2 Introduction

An alternative fuel or E-Fuel is one possible measure to reduce emissions of a traditional ICE. Such fuels absorb  $CO_x$  from the atmosphere during their production, so their overall carbon footprint is largely reduced [15, 11].

These alternative fuels can be used with conventional combustion engines to a certain extent, as the combustion process is, in principle, very similar. In practice, the combustion of such fuels has different requirements than the combustion of conventional fuels, which very often can't be met by the OEM motor.

The main challenge when converting an ICE to operate on alternative fuel comes from the injection system. Each fuel has different Air-Fuel Ratios (Air-Fuel Ratio (AFR)), which means a different amount of fuel has to be injected for the same operating condition compared to conventional fuels.

Most modern ECUs have built-in mechanisms to compensate for small changes in fuel composition, but fail when dealing with large differences. From the motorsport world, this is a very well-known problem, especially in the drag racing sphere, where race cars use highly modified fuels to achieve higher performance levels. A very common approach in this realm is to use a so-called "aftermarket" ECU, which gives complete control over the motor and more flexibility. Another way this can be achieved is by reprogramming the OEM ECU, which often involves hacking it, is not supported for all vehicles, and manufacturers actively take measures against this practice.

Such methods might be well suited for motorsport applications, but not for consumer vehicles, which rely on the ECU for functions other than motor control, and have other priorities beyond maximum performance. The goal of this project is therefore to investigate how feasible it is to create a module that can modify the injection control system to achieve a required mixture charge,

while still retaining a stock ECU and interfering as little as possible with other functionality.

# 3 Theoretical Background

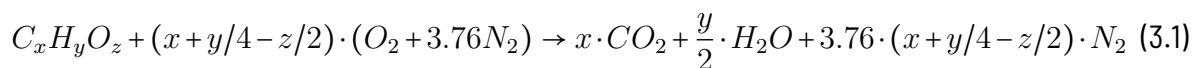
## 3.1 The Combustion of Alternative Fuels

To understand the requirements for the module, it is first necessary to analyze the combustion stoichiometry for the fuels in question.

Stoichiometric combustion is the complete oxidation of carbon and hydrogen in the fuel, resulting in carbon dioxide and water as the only products. The stoichiometric air-fuel ratio (AFR) is the ratio of air to fuel that achieves this complete combustion.

When using air for the combustion, and not pure oxygen, we must consider the nitrogen in the air, which does not participate in the combustion reaction. This means that the stoichiometric AFR is higher than it would be with pure oxygen.

General combustion of hydrocarbons can be described by the following equations [4]:



Where  $x$ ,  $y$ , and  $z$  represent the number of carbon, hydrogen, and oxygen atoms in the hydrocarbon molecule, respectively. The coefficient  $(x + y/4 - z/2)$  represents the amount of oxygen needed for complete combustion, and 3.76 is the nitrogen-to-oxygen ratio in air.

The oxygen demand for the stoichiometric combustion of the reactants can then be calculated as:

$$O_{dem} = x + \frac{y}{4} - \frac{z}{2} \quad (3.2)$$

The air-fuel ratio is the ratio of the mass of air to the mass of fuel required for stoichiometric combustion. It can be calculated using the molar masses of the components:

$$AFR = \frac{M_{air}}{M_{fuel}} \quad (3.3)$$

Where  $M_{air}$  is the molar mass of air,  $M_{O_2}$  is the molar mass of oxygen, and  $M_{fuel}$  is the molar mass of the fuel.

## 3.2 A Simple Model for Alternative Fuel Combustion

Professor Kaufmann was kind enough to provide an Octave model that can be used to compare the combustion of E-Fuels with conventional fuels. With the help of this model, fuel system requirements can be derived based on the combustion properties of the fuels.

### 3.2.1 Fuel and Air Properties

The model begins by defining the fundamental properties of air and various fuel components. Air is characterized by its composition (approximately 21% oxygen and 79% nitrogen by mole) and the respective molar masses of its components. From these values, important properties are derived:

- Average molar mass of air
- Mass composition of air
- Specific gas constant for air

For fuels, the model considers various hydrocarbon components that may be present in alternative fuels, including alkanes (heptane, octane), alcohols (methanol, ethanol), and other oxygenated compounds. Each component is defined by:

- Molecular formula ( $C_xH_yO_z$ )

- Molar mass
- Liquid density at standard conditions
- Enthalpy of formation

### 3.2.2 Stoichiometric Requirements

Based on the molecular formula of each fuel component, the model calculates the minimum oxygen demand using equation 3.2:

From this, the minimum air requirement is calculated by considering the oxygen content in air. The air-fuel ratio can then be determined based on the molar masses:

$$L_{min} = \frac{O_{min}}{\xi_{O_2}} \quad (3.4)$$

Where  $\xi_{O_2}$  is the mass fraction of oxygen in air.

### 3.2.3 Exhaust Gas Composition

The model accounts for varying air-fuel ratios by introducing the lambda ( $\lambda$ ) value, which represents the ratio of actual air to stoichiometric air.

$$\lambda = \frac{AFR_{actual}}{AFR_{stoich}} \quad (3.5)$$

For a given lambda, the model calculates:

- Actual oxygen and air requirements

- Exhaust gas composition ( $\text{CO}_2$ ,  $\text{H}_2\text{O}$ ,  $\text{N}_2$ , and excess  $\text{O}_2$  if  $\lambda > 1$ )
- Molar fractions of exhaust components (both wet and dry basis)

### 3.2.4 Fuel Energy Calculation

The heating value of the fuel is determined based on the enthalpy of formation of the fuel components and combustion products:

### 3.2.5 Engine Performance Calculations

For practical application, the model calculates the required fuel mass based on engine parameters such as displacement, mean effective pressure, thermal efficiency, and intake manifold pressure. The values are only an estimate, as they do not take into account gas dynamics or the multitude of other factors that can influence combustion in an engine [8].

Figure 1 shows the fuel demand for different types of fuels at various engine loads (Mean Effective Pressure).

Using the values from figure 1, we can estimate the increase in fuel demand when converting a gasoline system to an alternative fuel system. For methanol, an increase of approximately 86% is required, and for DMC around 95%.

## 3.3 Fuel Injection Systems and Injection control

The fuel injection system is responsible for delivering the fuel in the combustion chamber. It is therefore the main system that has to be modified for the use of alternative fuels.

Most modern motors use Electronic Fuel Injection (EFI) systems, which are controlled by the engine control unit ECU. Carburetors are still used in older motors, and will not be considered in the scope of this project.

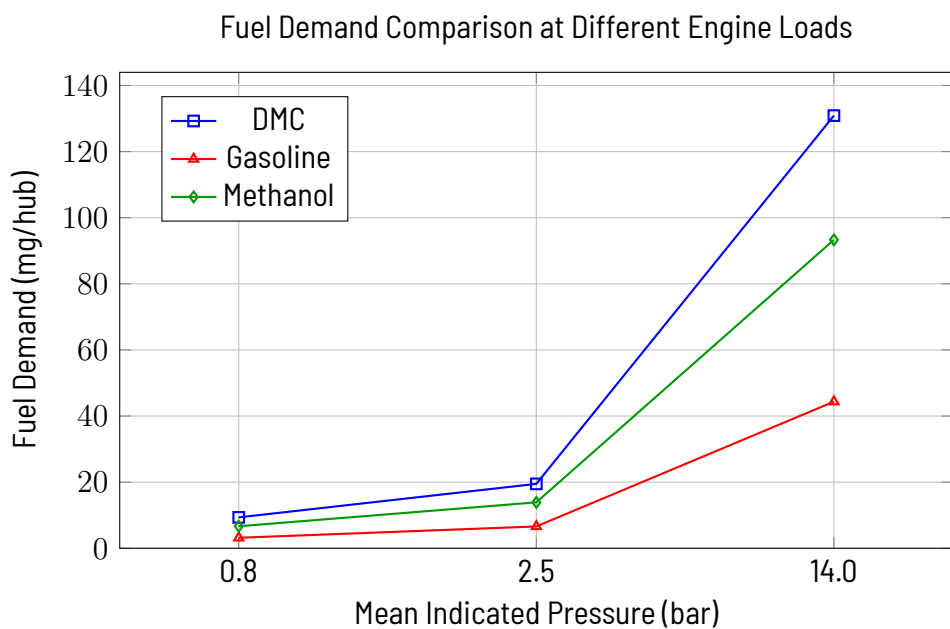


Figure 1: Comparison of fuel mass demand per hub for different fuel types at varying engine loads

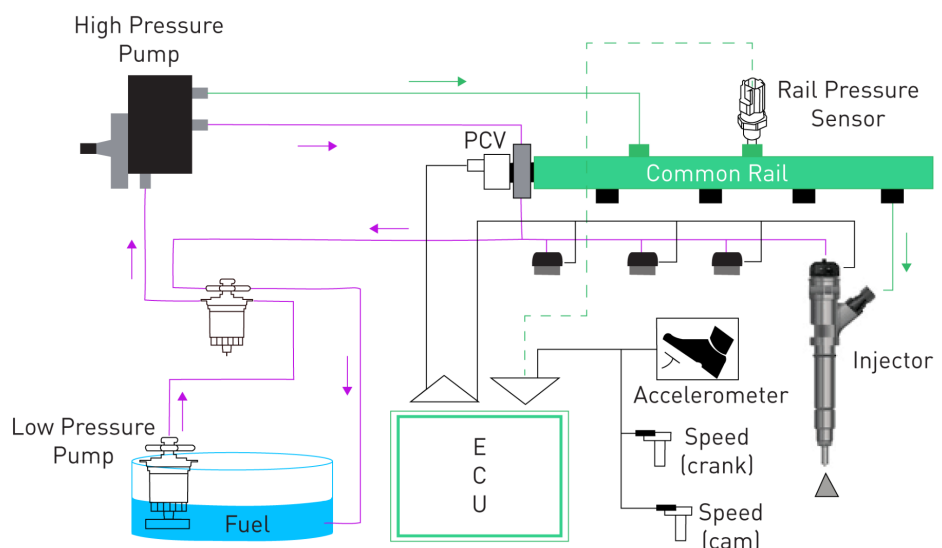


Figure 2: Fuel Injection System Overview. Adapted from [7]

We can distinguish between the two main types of fuel injection systems: port injection and direct injection [9]. Both rely on the injectors to deliver the fuel, but differ in how and where the fuel is delivered.

For this project, the more interesting aspect is, however, how the injectors are controlled. In a typical EFI system, the ECU sends a signal to the injector to open it for a certain amount of time, allowing the fuel to flow through the injector and into the combustion chamber. This time for which the injector is held open shall be referred to as the injection pulse width

The amount of fuel delivered is then only proportional to the injection pulse width, the fuel pressure on the rail, and the flow rate of the injector.

This project will focus only on the control of the injection pulse width to achieve the required fuel mass. The fuel rail pressure and injector flow rate will therefore be assumed to be constant.

## 3.4 Injector Driver Topologies

A typical fuel injector can be represented as a simple series RL circuit.

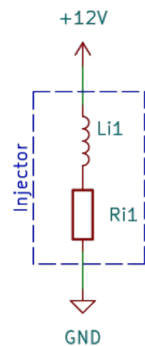


Figure 3: Injector as an RL Circuit

With the fundamental equation

$$V = L \cdot \frac{di}{dt} + R \cdot i \quad (3.6)$$

solving for current:

$$i(t) = \frac{V}{R} \cdot (1 - e^{-\frac{R}{L}t}) \quad (3.7)$$

It is clear from this simplified model that the current through the injector will rise when a voltage is applied, and will settle at a certain value, which is mainly limited by the resistance. If the injection pulse width is long enough, we can assume that the maximum current will be given by:

$$I_{max} = \frac{V}{R} \quad (3.8)$$

The injectors are controlled by the ECU through a driver circuit, which is responsible for providing the necessary current to open the injector. There are two main types of injectors: low impedance and high impedance.

Low impedance injectors require a higher current to open, while high impedance injectors require a lower current. The driver circuit must be able to provide the necessary current for the specific type of injector used.

High impedance injectors can be driven by saturation type injector drivers, and the maximum current across the injector will be given by the supply voltage and the DC resistance (equation 3.8).

Low impedance injectors can also be driven through peak and hold drivers. These work by first applying a high voltage to the injector to quickly reach the opening current, and then switching to current control mode to maintain the current at a minimum, while still holding the injector open. This is quite common in motorsport engines, where the injector opening time has to be minimized, which leads to the need for low impedance injectors, and peak and hold drivers.

It is important to note that a saturation injector driver will not be able to drive a low impedance injector. A peak and hold driver, on the other hand, can drive both low and high impedance injectors, at the cost of added complexity and expense.

For this project, the choice was made to use a peak and hold capable system, as it allows more flexibility when it comes to injector choice.

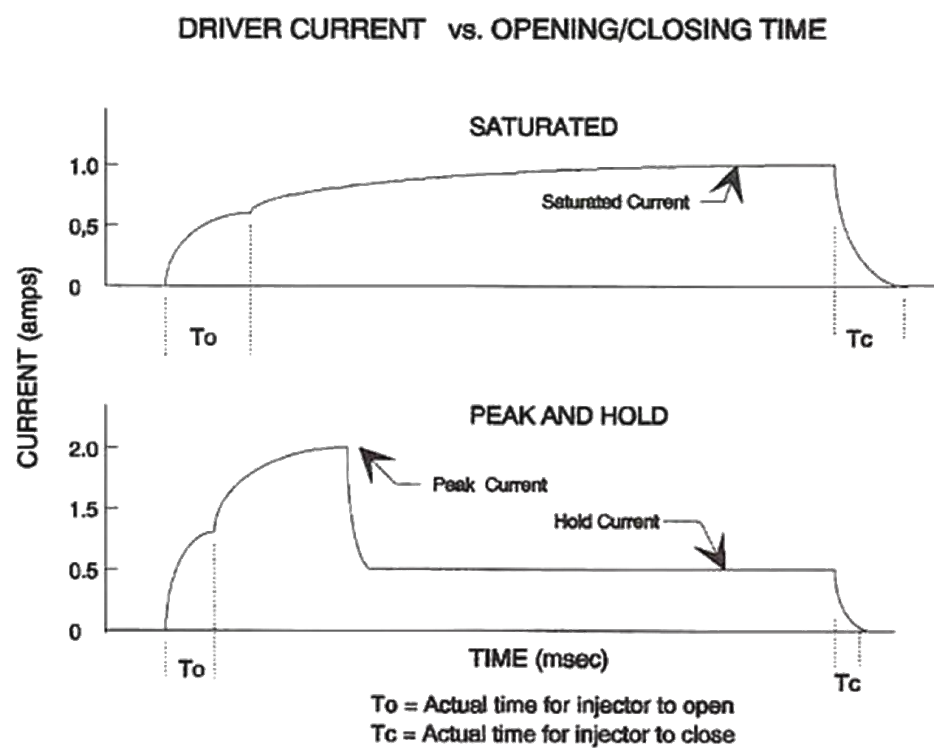


Figure 4: Comparison of Peak and Hold and Saturation Drivers. Adapted from [3]

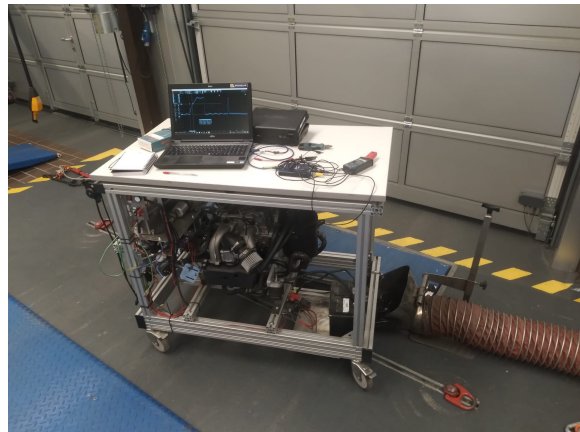
## 4 Preparation

The motor of choice used for the development and testing of the module is a Weber 2-cylinder 4-stroke spark-ignited motor with multipoint sequential injection (EFI).

The motor has a compression ratio of 9:1 and a displacement of 846 cm<sup>3</sup>. It is a naturally aspirated motor with a dry sump lubrication system. From previous projects at the RWU, the motor was mounted on a movable motor stand with all peripherals connected, including the fuel system, exhaust system, and electrical system. This specific motor was fitted with a Continental Easy-U1 WEBER ECU. Unfortunately, the diagnostic tool for the ECU was not available at the time of the project.



(a) Weber MPE 850 maritime motor. Adapted from  
[10]



(b) Motor ready for testing

Figure 5: Test motor and measurement setup for injector characterization

When inspecting the motor during the first tests, several issues were found. Some fuel lines had to be replaced due to small leaks, and the fuel pressure was not high enough, resulting in very lean combustion (the motor has no lambda closed loop control). The fuel pressure was adjusted

according to the motor installation manual to 4 bar [14]. The tachometer of the motor was also reading incorrectly, consistently showing exactly half of the real RPM. This could be due to the fact that the Weber motor does not use wasted spark on the ignition system. The motor RPM for the next measurements was deduced from the injection signal, which was measured with an oscilloscope.

The Innovate LM2 AFR meter that had been used in previous tests also malfunctioned, so it could not be used for the measurements. A MAHA MET 6.3 emission tester was used instead.

Having the motor at hand, the next step was to characterize the injectors and the ECU injector driver. This was done by measuring current and voltage at the injectors' terminals in different operating conditions. From these measurements, the DC resistance and inductance of the injectors were estimated, which are crucial parameters for the module design.

It is important to note that the injector parameters are also needed to emulate the injectors for the ECUs to accept the modification. Modern ECUs have diverse diagnostic mechanisms to ensure that the multiple systems in the motor are functioning properly, including the injectors. Upon testing, it was found that for the specific ECUs used in the Weber motor, the control unit only needs to have a resistance of similar value to that of the injector, and no inductance is required. This means that the module can be designed to emulate the injectors as resistors, which simplifies the design. The resistors will have to dissipate a considerable amount of power, depending on the duty cycle of the injectors (analogous to the injection pulse width), so they will have to be chosen accordingly.

## 4.1 Injector Characterization

The current was measured with a TA018 Current Clamp (60A AC/DC) connected to a PicoScope 2204A PC Oscilloscope, and the resistance was measured using a Fluke 1279 TRUE RMS Multimeter. The measurements were conducted with the motor running at different RPMs and various injection pulse widths. All measurements were performed with the battery voltage stable at approximately 12 V to ensure consistent results.

In Figure 6, some noise due to the motor's other peripherals is visible, but the general trend is clear. The injector current (in blue) rises for approximately 1 ms up to a visible peak, and then continues to rise until reaching the saturation value. This intermediate peak denotes the opening time of the

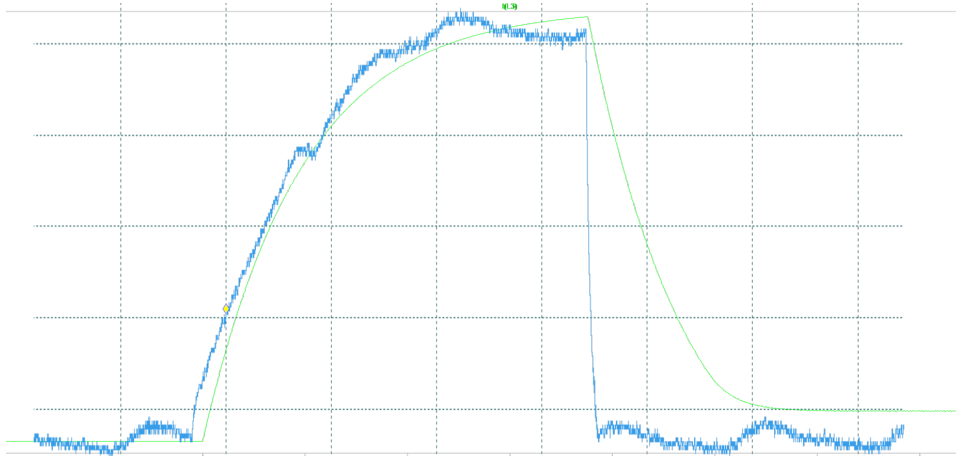


Figure 6: Injector Characterization: measured current (blue) vs simulated current (green)

injector [17]. It can also be confirmed that the injector is a high-impedance injector (around  $12\ \Omega$ ), as the current does not rise above 1 A with a driving voltage of 12 V.

The inductance of the injector can be calculated from the first time constant of the current rise, which is the time it takes for the current to rise from 0 to 63.2% of its final value. For an RL circuit with a step voltage input:

$$\tau = \frac{L}{R} \quad (4.1)$$

From the measured values, an inductance of approximately 12 mH was estimated. This is based on multiple measurements of the first time constant, which ranged from 817  $\mu\text{s}$  to 1216  $\mu\text{s}$ , with an average DC resistance of  $12.3\ \Omega$ . These values are in line with the literature for similar injectors [17][13][6].

Table 1: Injector Characterization Measurements

<b>R (Ω)</b>	<b>I<sub>max</sub> (mA)</b>	<b>τ (μs)</b>	<b>L (mH)</b>	<b>T<sub>open</sub> (ms)</b>	<b>T<sub>high</sub> (ms)</b>
12.3	891.4	817.2	10.05	1.197	3.779
12.3	895.5	1216.0	14.96	1.180	3.758
12.3	896.0	1059.0	13.03	1.174	3.766
12.3	892.0	930.6	11.45	1.170	3.747
12.3	883.0	981.6	12.07	1.176	3.788
12.3	817.7	993.0	12.21	1.263	3.543
12.3	783.2	970.1	11.93	1.277	3.034
<b>Average</b>	<b>865.5</b>	<b>995.4</b>	<b>12.24</b>	<b>1.205</b>	<b>3.631</b>



Figure 7: Inductive Kickback from the Injector

The measured opening time of the injectors was consistently around 1.2 ms, which corresponds to the visible peak in the current profile [17]. This observation further supports the hypothesis that the injectors in the Weber motor are high-impedance injectors, as low-impedance injectors typically have a much shorter opening time.

From Figure 7, we can also make conjectures about the driver in the ECU. The current drops drastically after the injector is shut off, which indicates that the driver employs an active clamping topology. This rapid demagnetization time ( $T_{DEMAG}$ ) is an important parameter for injector control.

The demagnetization time in an inductive circuit can be calculated by solving for when the total current decays to zero [12, 5].

$$T_{DEMAG} = \frac{L}{R} * \ln\left(1 + \frac{R * I_0}{V_{CLAMP} - V_{BAT}}\right) \quad (4.2)$$

Where:

- $L$  is the inductance of the injector
- $R$  is the resistance of the injector
- $I_0$  is the initial current at turn-off
- $V_{CLAMP}$  is the clamping voltage
- $V_{BAT}$  is the battery voltage

The rapid decay observed in the measurements indicates a relatively high clamping voltage compared to the battery voltage, which effectively reduces demagnetization time. The downside of such a high clamping voltage is that the injector driver output stage needs to handle higher avalanche power (energy released by the collapse of the magnetic field in the inductor).

# 5 Prototype Design and Construction

## 5.1 Technical Requirements

The main goal of the project is to create an interface between the ECU and the injectors that enables the use of alternative fuels by modifying the injection pulse width. After careful consideration, the following technical requirements were set:

- **Power Supply:** Operation from a standard automotive 12V system (lead-acid battery)
- **Injection Detection:** Accurate detection of start of injection (SOI) and end of injection (EOI) signals from the ECU with precise measurement of the pulse width
- **Pulse Width Extension:** Ability to extend the injector "ON" time by an adjustable percentage to accommodate different fuel requirements
- **Installation:** Positioned between the ECU injector driver and the injector solenoid, completely isolating the injector from the ECU
- **ECU Compatibility:** Emulation of the injector impedance characteristics to prevent detection by the ECU diagnostic systems
- **Power Management:** Efficient dissipation or reuse of the injector power signal from the ECU
- **Multi-cylinder Support:** Compatibility with various injection system configurations and firing orders, supporting up to 6 cylinders

- **Injector Drive Control:** Support for Peak and Hold operation mode with adjustable peak time and PWM frequency for current control

## 5.2 System Architecture

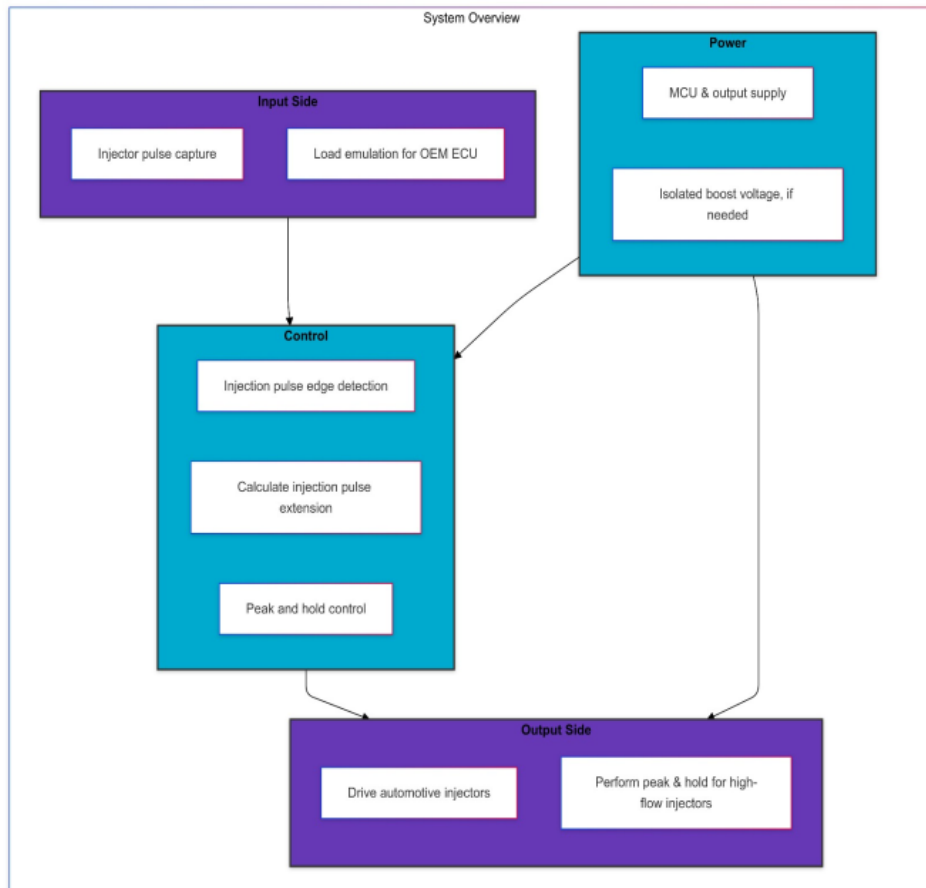


Figure 8: Block Diagram of the Prototype System

The requirements above led to a design that can be split into 4 main functional groups:

- **Input Block:** Captures the Start of Injection (SOI) and End of Injection (EOI) signals from the ECU, ensuring accurate timing for pulse width measurement.
- **Power Management Block:** Manages the Microcontroller Unit (MCU) power supply and the injector driver power supply.

- **Control Block:** Unlike previous designs that have used a full analog approach to manipulating the injection pulse width, this design uses a MCU to control the pulse width extension, the current control, and all other parameters of the injection pulse. At the expense of higher complexity, this approach allows for much greater flexibility, which is essential for adapting the module for different injection systems.
- **Output Block:** As complete isolation between the ECU and the injectors is required, the module must also have the necessary hardware to drive injectors. This is realized by a peak and hold capable injector driver.

### 5.2.1 Input Block

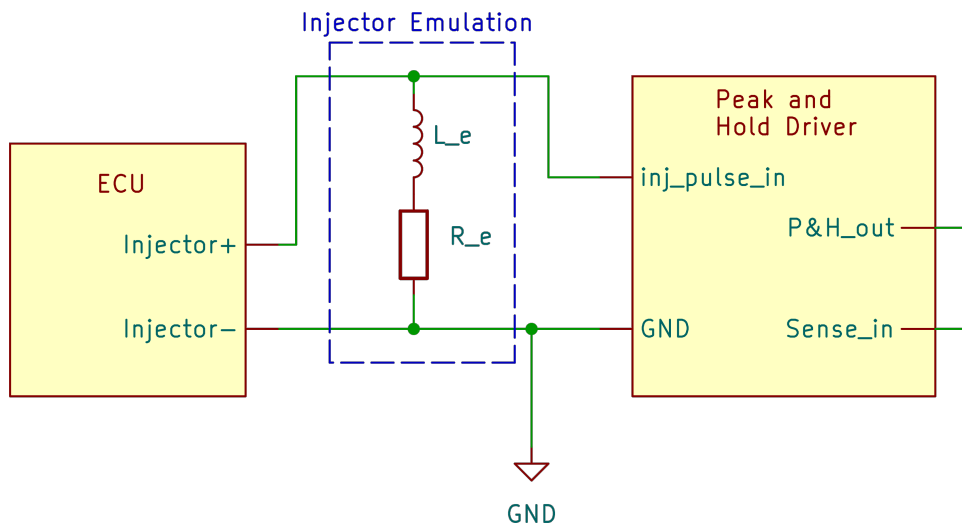


Figure 9: Input Block Diagram

The main function of the input block is emulating the injector impedance for the ECU. Different ECUs have different diagnostics for injector parameters, and no solution can be guaranteed without testing on the specific version of the ECU. For the Continental Easy - U1 WEBER ECU, the initial plan was to emulate the injector impedance with a resistor and an inductor in series, to achieve a similar impedance curve to that of the injector. However, upon testing, it was found that a simple  $12\Omega$  resistor is sufficient to prevent errors. Further testing is necessary to evaluate if this is a long-term solution, and if it could be generalized for other ECUs.

In any case, the power from the ECU injector driver must be dissipated or reused. For this proof of

concept prototype, a simple power resistor will be used to dissipate the power as heat, but future designs could use a more efficient solution to reuse the power.

## 5.2.2 Power Management Block

To simplify the design, it was decided to use the 12V battery power to supply the mosfets and the respective mosfet drivers. For the microcontroller, a 12V to 3.3V stepdown converter was used. The microcontroller can also be powered through USB, greatly simplifying the first prototype. Special care has to be taken against the reverse polarity of the power supply, as other typical hazardous situations in automotive applications (ISO 16750-2 and ISO 7637-2 describes several conditions that can lead to electrical failure in such an environment). Fuses and TVS diodes are used to protect the circuit from some of these events.

The TVS diode provides a low impedance path to ground for any voltage spikes, protecting both the logic inputs and the power terminals of the components from overvoltage.

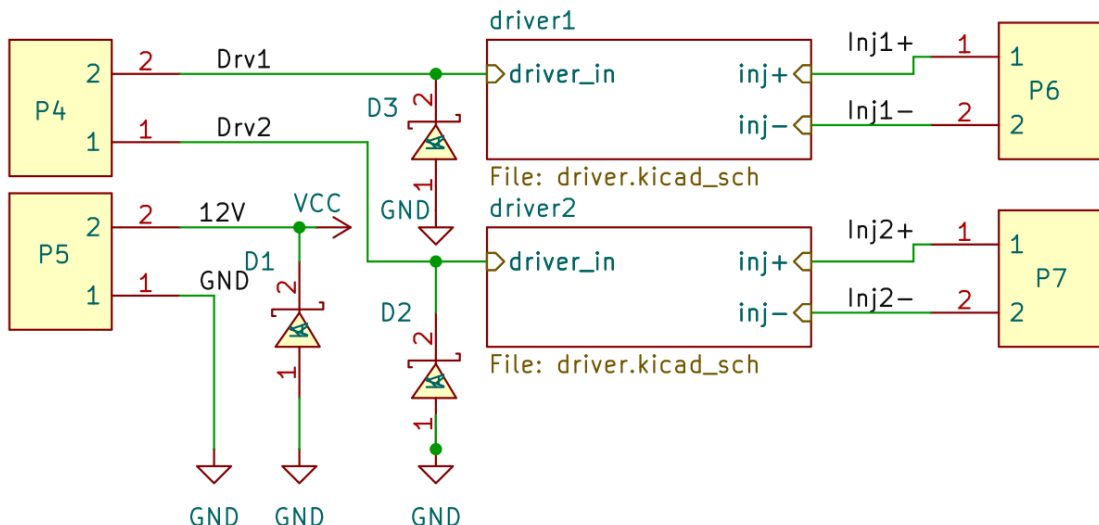


Figure 10: TVS Diode protection on logic inputs and power terminals

In the future, the input side can be combined with the power block to reuse the power from the ECU injector driver, improving overall efficiency.

### 5.2.3 Control Block

The digital logic is realized through an ARM Cortex-M4 microcontroller, which handles the timing of the injection pulse width

The logic can be summed up as follows:

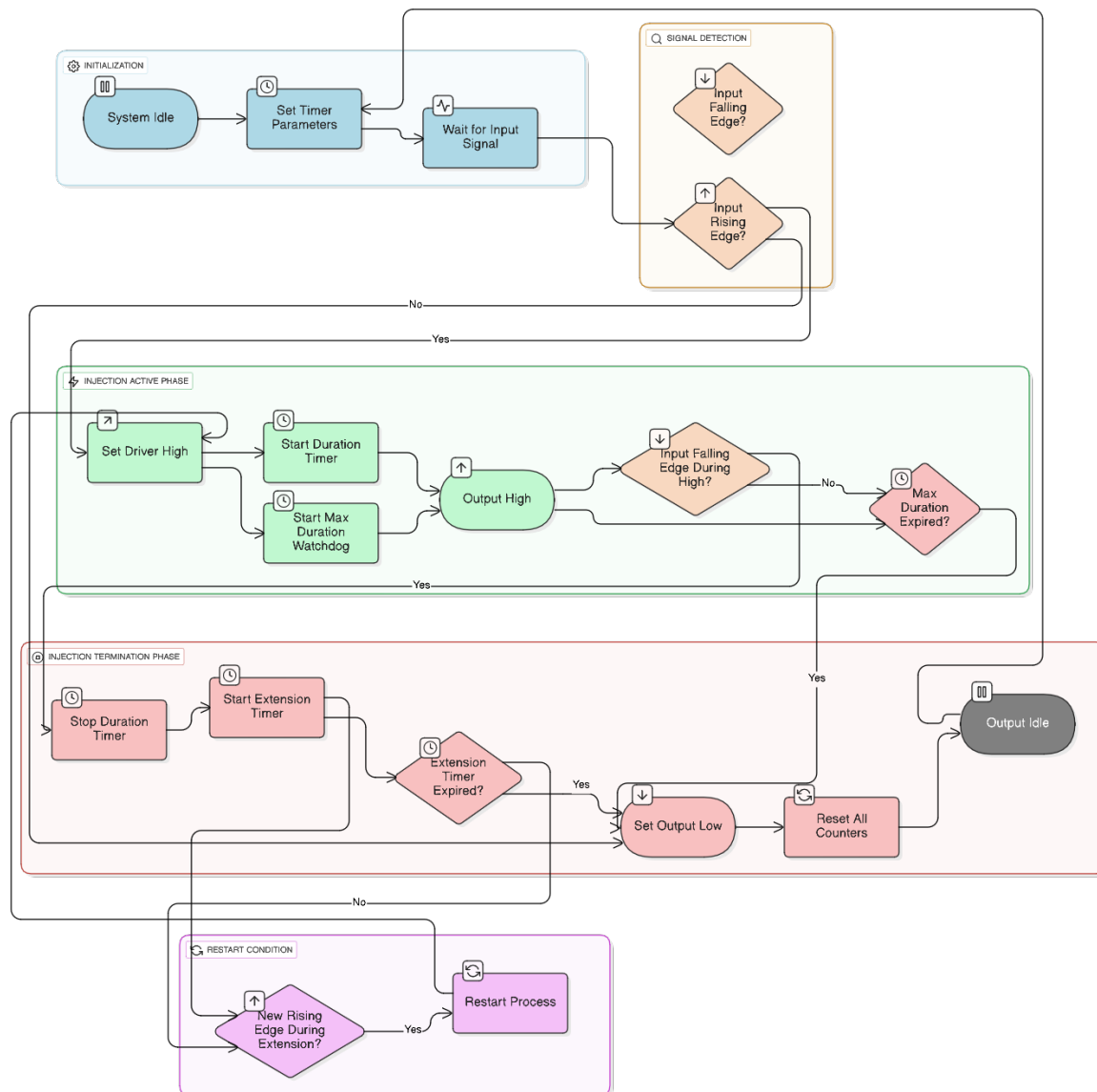


Figure 11: Control Logic Flowchart

The Cortex-M4 was chosen for its good clock speed, abundant peripherals, and most importantly, multiple timers. The digital logic was implemented in C, with focus on real-time performance, with a deterministic approach. At 7000RPM, each crank rotation takes approximately 8.57ms, which means on a 4 stroke engine, only 4.3ms are available for the fuel to be injected. This is the so-called "injection window". At wide open throttle, the injector uses almost the entire injection window, up to 4.0ms to inject fuel. The system must be able to react to an input fast enough to ensure that the injection still takes place inside the injection window.

All core functionalities run on timer interrupts. With the detection of an injection event, a series of timers are started to control the injection process, and the peak and hold functionality, along with failsafes to prevent catastrophic failure. This highly deterministic approach is essential for an application like this.

Several failure cases were considered, the most dangerous being pre-ignition of the mixture due to badly timed injection events, and uncontrolled injection, leading to the "flooding" of the cylinder.

The latter could lead to the cylinder being filled with fuel while the motor is still off, and "lifting" the cylinder head when starting the motor (phenomenon known as "hydraulic lock"). To prevent this, the module has a failsafe that will stop the injection process if the injection pulse width exceeds a certain threshold (see Figure 11), which can be adjusted by the user. The code was also written in a manner that the output is normally low (that is, default output state is low).

A failure to detect and react to an ECU input in time could also lead to incomplete combustion, not giving the fuel time to undergo atomization properly. The bare-metal timer approach allows for a highly deterministic execution time, which minimizes the risks of this happening.

## 5.3 Output Block

The output block design is, from a hardware point of view, the most critical part of the system, as it has to handle the high injector currents and the high kickback voltage resulting from the inductance of the injector.

The output block was designed independently from the control block, to improve flexibility. Each output module has two injector outputs, and they can be used in parallel with a single control block

to drive as many injectors as the control module can handle.

The output injector driver circuit is also driven directly from the 12V battery system, which negates the need for more power blocks when adding more output modules. This results in a fully modular system, that can be expanded to accommodate different injection system requirements.

To achieve peak and hold operation, there are several approaches that can be used. A dual voltage supply can be used, with a high voltage to achieve the peak current, and a lower voltage for the hold phase. This, however, adds complexity, as it requires a boost converter for the high voltage, and a stepdown for the hold voltage.

Another approach is to use a peak and hold driver IC, such as the Texas Instruments LM1949 [13], which is designed specifically for this purpose.

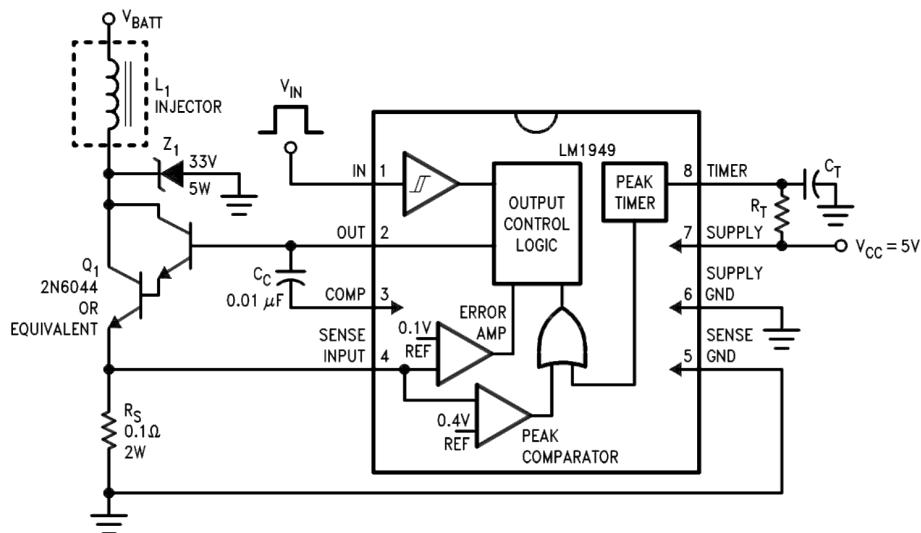


Figure 12: LM1949 Application Circuit. Adapted from [13]

The LM1949, however, relies on a transistor operating in its linear region for the current control. This leads to high power dissipation and unnecessary losses on the driver. It can also be operated in a PWM mode, but this requires the PWM parameters to be set on a hardware level, which goes against the design philosophy of keeping the module as flexible as possible.

For this sake, it was decided upon a custom peak and hold driver, which uses a low side N-channel power MOSFET to control the injector current. The current control is realized through a high fre-

quency PWM signal, which is generated by the MCU PWM timers. This simplified digital logic approach allows for maximum flexibility, as the PWM parameters can be adjusted in real-time through the MCU.

The circuit was also designed to be normally open, that is, the output will be low by default, so in case of failure, the output will be low, which means the injectors stay closed. TVS diodes are also used to protect the input from overvoltage spikes, as well as the MCU from the inductive kickback. A voltage follower circuit was also added to the MCU outputs to guarantee isolation between logic and power circuits, preventing the high currents from affecting the MCU operation.

Later, input optical isolation had to be added to the circuit. The "Easy - U1 WEBER" ECU uses an isolated ground for the injectors, not connected to the battery ground. This means that the input signals from the ECU must be isolated from the output signals to prevent ground loops and ensure proper operation. An optocoupler was added to the input side of the circuit to provide this isolation, at the cost of increased complexity and latency (in the microsecond range, still very tolerable for the application).

### 5.3.1 Current Control

When switching a voltage across an inductor, if the switching frequency is high enough, the current will be constant, and controlled by the duty cycle of the PWM signal.

If the voltage is switched on and off at a high frequency, the average current can be controlled by the duty cycle  $D$  of the PWM signal:

$$I_{avg} = D \cdot \frac{V}{R} \quad (5.1)$$

where  $R$  is the resistance of the inductor.

The so-called "hold" current, that is, the minimum current to hold the solenoid open, should be measured on an experimental basis for each injector type.

The peak current should be set to a value that is high enough to open the solenoid consistently.

Due to the lack of data on the injectors on the Weber motor, and the lack of an adequate dedicated

injector testbench to evaluate their performance, it was decided to drive the injectors on the Weber motor in saturation mode, just like the OEM ECU does.

### 5.3.2 Kickback Protection

When the current through an inductor is suddenly interrupted, the inductor will try to maintain the current flow, leading to a voltage spike given by:

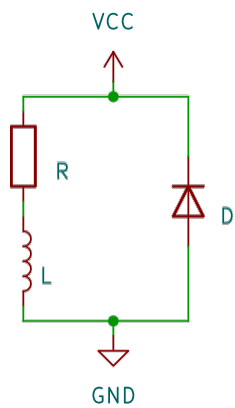
$$V_{kickback} = L \cdot \frac{di}{dt} \quad (5.2)$$

where  $L$  is the inductance of the load and  $\frac{di}{dt}$  is the rate of change of current.

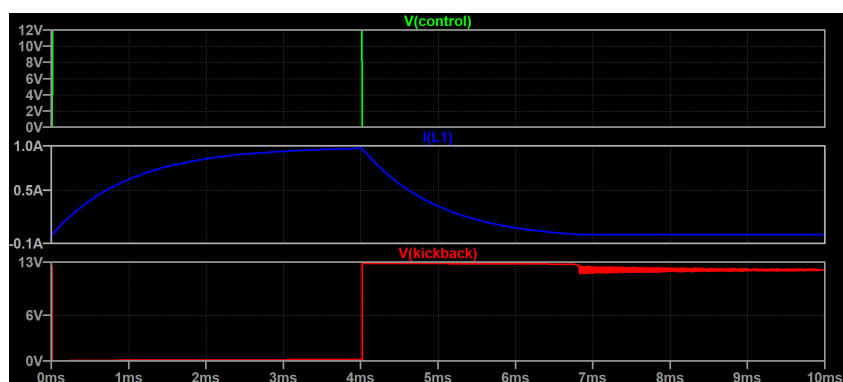
This voltage spike is called inductive kickback, and can damage driving circuitry if not mitigated. The simple way to dissipate this energy is to provide a low impedance path to ground for the current to flow when the MOSFET is turned off. Two main solutions were considered: a freewheeling diode clamp and a Zener diode clamp.

#### Freewheeling Diode

The simplest approach is to use a freewheeling diode, which provides a path for the current to flow when the MOSFET is turned off. This diode should be rated for the maximum current and power dissipation of the injector.



(a) Freewheeling diode circuit schematic



(b) Simulated waveforms showing inductor current and voltage

Figure 13: Freewheeling diode implementation for inductive kickback protection. The diode provides a path for the current to flow when the MOSFET switches off, limiting the voltage spike across the inductor.

### Zener Clamp

A disadvantage of the simple freewheeling diode is that due to the low forward voltage of the diode and the internal resistance of the solenoid, the dissipation current will be very limited. For an injector with  $12\ \Omega$  of DC resistance, and a forward voltage of 0.7 V, the current will be limited to approximately 0.06 A, which is not enough to quickly dissipate the energy stored in the inductor. This results in a slow decay of the current, which increases the shutoff time of the injector.

Adding a Zener diode in series with the freewheeling diode can help to increase the voltage drop across the diodes, while still protecting the MOSFET from too high voltages. The Zener diode will clamp the voltage spike to a safe level, allowing the current to flow through the freewheeling diode and dissipate the energy stored in the solenoid as quickly as possible.

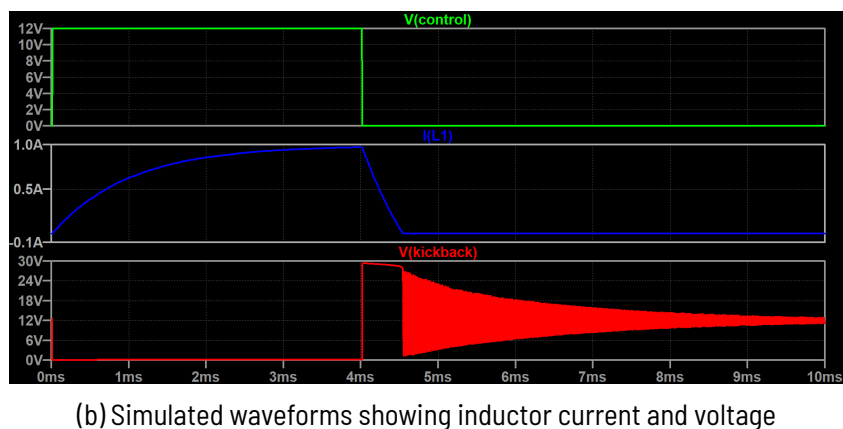
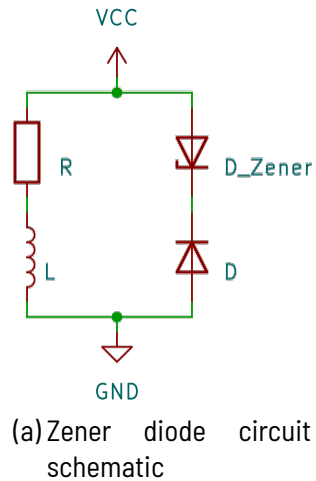


Figure 14: Zener diode implementation for inductive kickback protection. The Zener diode clamps the voltage spike, protecting the MOSFET from high voltages.

For the prototype, the Zener approach was chosen. Care must be taken when choosing MOSFETs and Zener diodes to ensure that the Zener clamp voltage won't overcome the MOSFET's rated breakdown voltage, which could lead to catastrophic failure of the driver circuit.

### FET Ringing Mitigation

As can be seen in figure 14b, when increasing the clamping voltage, the ringing of the MOSFET gate can become more pronounced, resulting in ringing on the output, visible in the voltage waveform. According to the Toshiba Electronics application note on the topic [16], when the MOSFET turns off, the  $di/dt$  of the drain current and the stray inductances of the drain lead and wire cause a voltage surge across the drain and the source. This surge voltage is expressed as [16]:

$$V_{\text{Surge}} = L_{S2} \times \frac{di}{dt} \quad (5.3)$$

When the diode in the drain-source loop is in conduction (i.e., energy from L is being recirculated), the circuit causes ringing since the surge voltage resonates with the  $C_{ds}$  of the MOSFET and the stray inductance  $L_{S2}$ . Since the impedance of C1 is sufficiently low for parasitic oscillation frequency, it can be considered to be short-circuited [16].

The surge voltage is superimposed on the  $v_{GS}$  voltage via the gate-drain capacitance  $C_{gd}$  of the MOSFET. As a result, it might also affect the gate inductance as shown in Figure 15, causing ringing of the gate voltage.

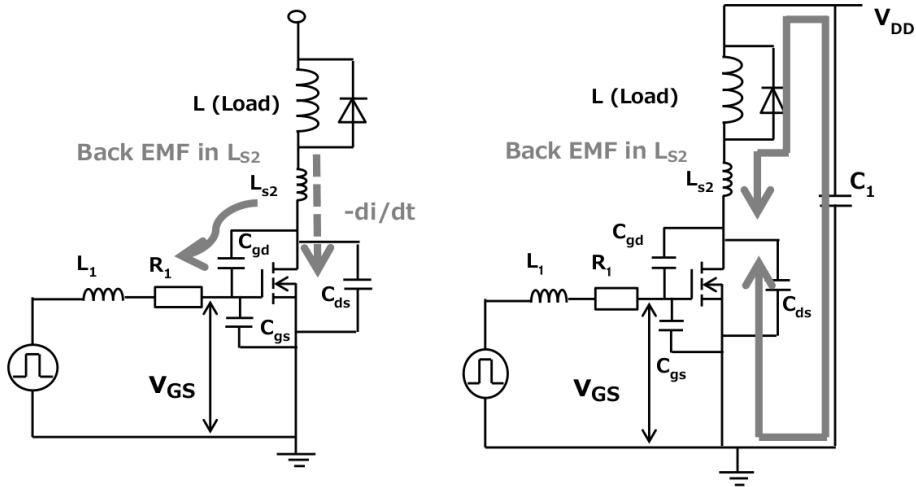


Figure 15: Positive Feedback Paths when Driving Inductances. Adapted from [16]

This FET ringing can be mitigated in several ways. For this application, a simple gate resistor was used, which will limit the  $di/dt$  of the gate voltage, at the cost of a slightly slower turn on time of the MOSFET.

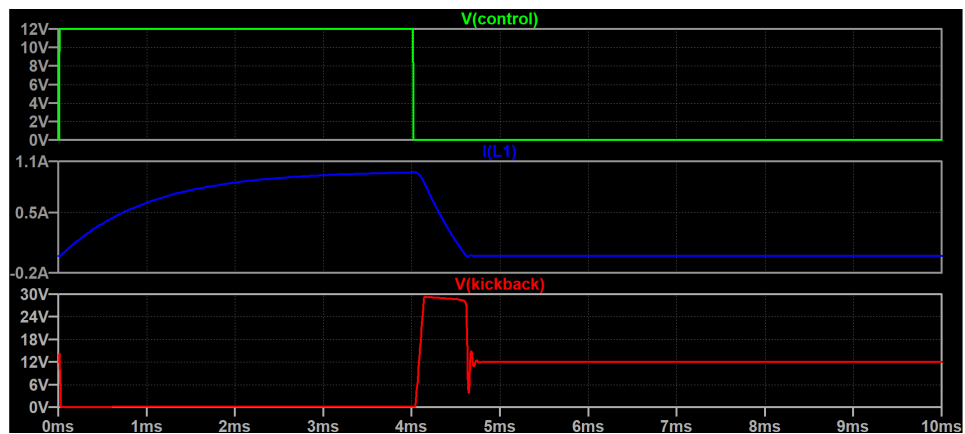


Figure 16: Simulation results with the added gate resistance: reduced ringing.

The proposed solution was designed with SPICE, and later validated on the real hardware.

## 5.4 Prototype Construction

A custom two-sided PCB was designed in KiCad to accommodate all the output driver components. The PCB was designed with a double-sided layout, with both a ground plane and a power plane for noise rejection purposes. A small optical isolation board was hand soldered, along with a development board for the MCU. The reason for separating the system into several boards was to allow for easier replacement of parts in case of failure, and more adaptability. The complete system block diagram can be seen in figure 17.

The prototype boards were also pre-assembled by the PCB manufacturer. Due to the mosfets operating in PWM mode only, thermal dissipation is not a problem, and no heatsinks were required.

A prototype system for the 2 cylinder Weber motor was assembled in a small enclosure, with the injector driver, power supply, MCU and a potentiometer to adjust the injection pulse width extension rate. Later, the optical isolation module was assembled on a prototype board, also added to the enclosure.

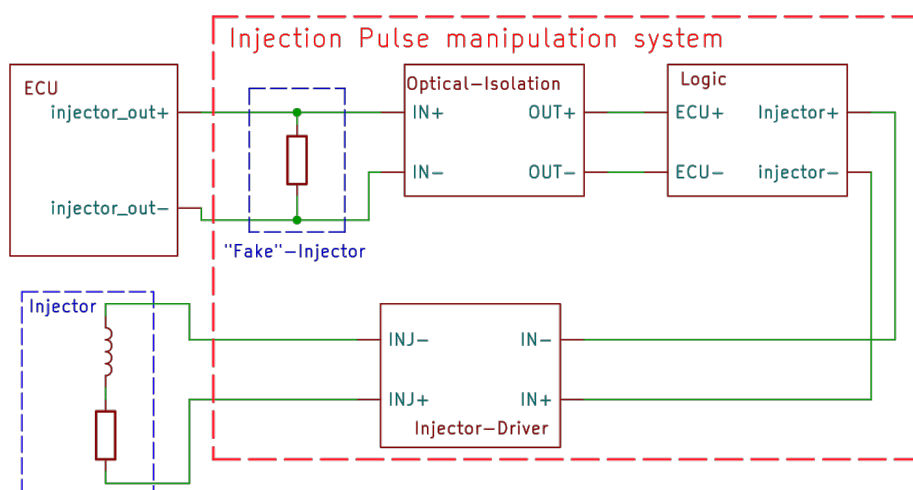
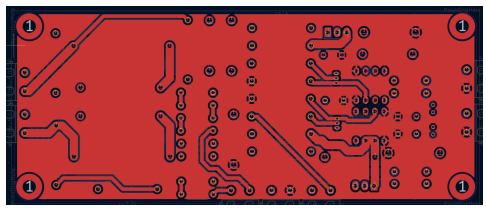
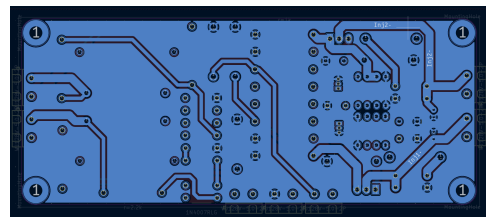


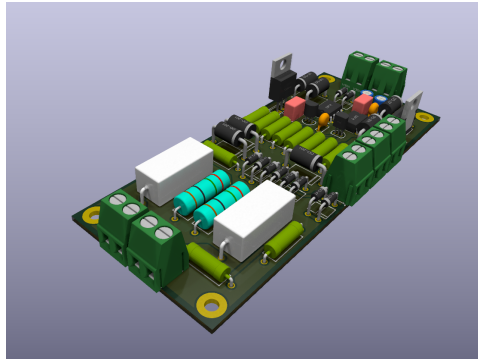
Figure 17: Complete System Block Diagram



(a) Injector Driver Back Copper



(b) Front Copper



(c) Driver Module 3D Render



(d) Complete System

Figure 18: PCB Design for the Peak and Hold Injector Driver: (a) Back copper layer with short traces for high current paths, (b) Front copper layer with control circuitry, (c) 3D rendered view showing component placement (d), Enclosure with all components ready to be mounted on the motor

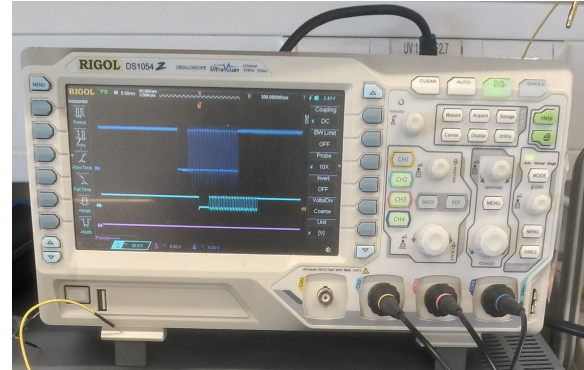
# 6 Prototype Testing

## 6.1 Testbench Testing

The prototype system was first tested on a testbench with a “dry” injector (injector without fuel flow) of similar specifications. The goal of these tests was to verify the correct operation of the peak and hold driver and to test the safety mechanisms of the system, especially on the software side.



(a) Dry injector testing



(b) Peak and hold timing test

Figure 19: Testbench setup for peak and hold driver testing

### 6.1.1 Injector Driver Operation

Initially, only the injector driver board was tested. The board was tested from 10V to 15V with a lab bench power supply, and the input signal was provided by a function generator.

The main goal of these tests was to verify the protection of the driver when driving inductive loads, along with current control. The driver was tested at different duty cycles and switching frequencies

over the mentioned supply voltage range. The input signal amplitude was also varied between 2.0 V and 5 V to verify the input signal threshold (the Cortex-M4 MCU has a 3.3 V logic level output).

The peak and hold operation of the driver was also validated at this stage, but the results are limited. Without an injector testbench, the actual flow of the injector cannot be measured, so it cannot be verified if the injector was being held fully open. The results are therefore merely qualitative, showing that the driver can hold the current across the inductor inside a threshold.

### 6.1.2 Logic Edge Case Testing

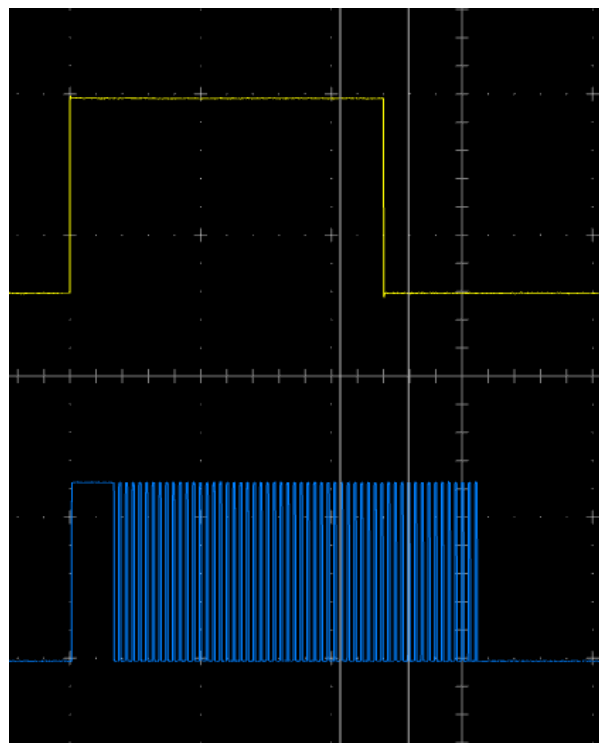


Figure 20: Input Saturation pulse and Output Peak and Hold PWM signal

Several critical situations were tested. The most important were the behavior when turning on the driver, turning off the driver, unexpected shutdowns, missed input rising or falling edges, and changing parameters during operation.

The results were checked by analyzing the output signal from the control module with an oscilloscope and comparing it to the expected signal. The phase delay between input and output was also

measured, and a Worst Case Execution Time (WCET) of approximately  $50 \mu\text{s}$  was observed, which is acceptable for the application.

During this stage, an issue was found when changing the PWM frequency of the current control during operation. This was due to an interrupt updating a timer register getting preempted by the current control interrupt, which would then read from the same register. This was fixed at the software level by adding a flag to protect the resource from concurrent access.

After this stage, the driver was ready to be tested live on the motor.

## 6.2 Testing on the Weber motor

The prototype system was then tested on the Weber motor. The goal of these tests was to verify the correct operation of the system and to confirm the possibility of changing the fuel mixture through the module.

The module was mounted between the ECU and the two injectors on the motor.

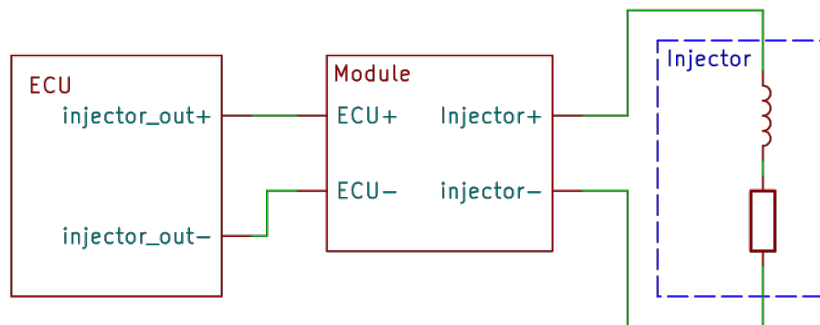


Figure 21: Connection between module, ECU, and injectors

Through the potentiometer, it was possible to increase the duty cycle of the injector driver and thus increase the amount of fuel in the mixture. This resulted in a change in the lambda value measured in the exhaust.

To validate the experiment, it's important to understand the mathematical relationship between the injector pulse width, Air-Fuel Ratio (AFR), and lambda ( $\lambda$ ). Assuming the air mass stays con-

stant (which is usually true unless boost or throttle position changes), we can establish several relationships:

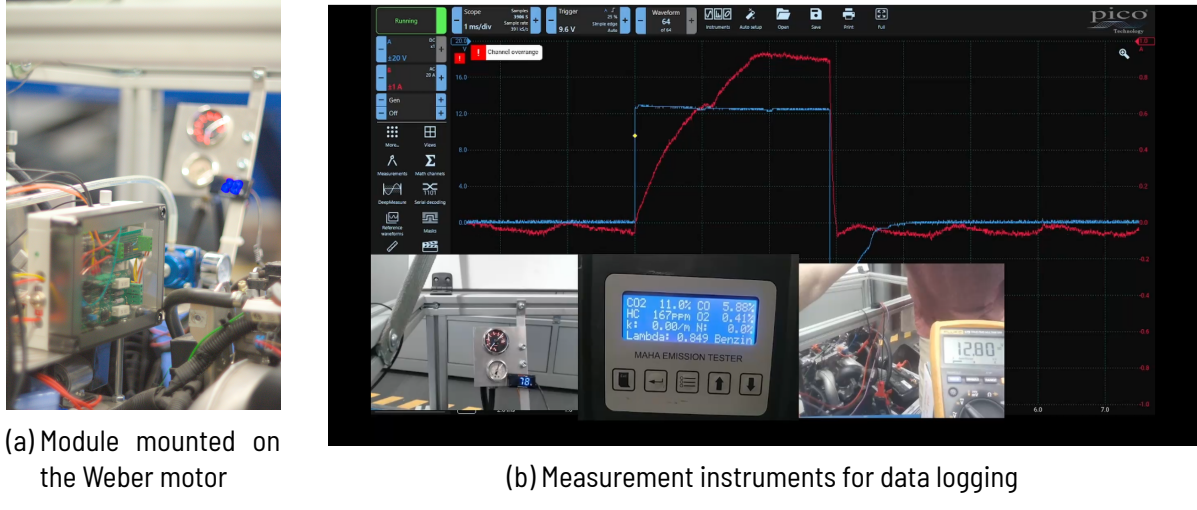


Figure 22: Testing the prototype module on the Weber motor

## Basic Definitions

**Pulse Width (PW):** The injected fuel mass is proportional to the injection pulse width. With a pulse width increase by  $x\%$ , the new fuel mass can be calculated as:

$$\text{Fuel}_{\text{new}} = \text{Fuel}_{\text{original}} \times \left(1 + \frac{x}{100}\right) \quad (6.1)$$

**Air-Fuel Ratio (AFR):** The ratio of air mass to fuel mass:

$$\text{AFR} = \frac{\text{Air mass}}{\text{Fuel mass}} \quad (6.2)$$

Assuming air mass remains constant, with an increase in fuel mass, the new AFR becomes:

$$\text{AFR}_{\text{new}} = \frac{\text{AFR}_{\text{original}}}{1 + \frac{x}{100}} \quad (6.3)$$

**Lambda ( $\lambda$ ):** The ratio of actual AFR to stoichiometric AFR:

$$\lambda = \frac{\text{AFR}_{\text{actual}}}{\text{AFR}_{\text{stoich}}} \quad (6.4)$$

Finally, when AFR changes due to pulse width increase:

$$\lambda_{\text{new}} = \frac{\lambda_{\text{original}}}{1 + \frac{x}{100}} \quad (6.5)$$

## Results

For example, with a 10% increase in pulse width, assuming an original stoichiometric mixture ( $\lambda = 1$ ):

$$\lambda_{\text{new}} = \frac{1}{1.10} \approx 0.909 \quad (6.6)$$

This creates a richer mixture (lower lambda value).

A lambda sensor was used to measure the exhaust composition after the collector (where the exhaust gases from both cylinders mix). The motor was run on normal pump gasoline for these tests. By observing changes in lambda values proportional to the increase in the duty cycle, we can validate the effectiveness of the module in adjusting the fuel mixture.

The motor was run at idle with no load (throttle position at 0%). The exhaust composition was measured with a MAHA MET 6.3 emission tester, which provides real-time lambda values. It is important to note that due to technical issues, it was impossible to log the values, so they were recorded on video and later extracted from the video frames. The duty cycle extension percentage was held constant for 30 seconds before each measurement. The motor had no lambda feedback control, so the lambda value was expected to change proportionally to the increase in duty cycle. The injection driver was also operated in saturation mode, just like the original Weber injection driver.

Table 2: Expected Lambda Values vs Measured values for Different Duty Cycle Increases (Average of 3 measurements)

<b>Original Lambda</b>	<b>New Lambda</b>	<b>Duty Cycle Increase (%)</b>	<b>Expected Lambda</b>
0.839	0.795	5%	0.799
0.833	0.776	7%	0.778

As can be seen from Table 2, the measured lambda values are relatively close to the expected values. It must also be noted that even though the motor does not have lambda closed-loop control, the ECU might still adjust the fuel mixture based on the RPM and other parameters, which can lead to inaccuracies. Increasing the duty cycle over 10% resulted in the ECU adjusting the duty cycle, which would invalidate the measurement.

The most important takeaway from this experiment, however, is that the whole system can be integrated into an existing fuel injection system, manipulate the mixture in real time, and remain undetected by the ECU.

The reliability of the pulse detection was also verified during these tests. Over 192 recorded pulses, none were missed. The average reaction time from the system was consistently under  $300\mu s$ , which is within the tolerable range for the application.

# 7 Conclusion

## 7.1 Summary of Key Findings

This thesis has demonstrated that fuel mixture control on an EFI motor is achievable through a non-intrusive approach. By intercepting and extending ECU injection signals, the tested prototype provides a practical solution for manipulating fuel injection without extensive modification to the injection system, or ECU reprogramming.

Testing has confirmed that the peak and hold driver design successfully operates with high impedance injectors. The implementation of digital logic for signal processing and timing control proved to be adequate, offering the necessary precision and flexibility for this application.

The predicted relationship between injection pulse width and lambda values was validated through experimental testing, confirming the theoretical foundation of the system's operation. These findings support the viability of the module as a potential solution for alternative fuel adaptation.

## 7.2 Accomplishment of Requirements

The developed system successfully met all primary requirements defined at the start of the project:

- **Peak and Hold operation:** The driver circuit effectively implements the peak and hold current profile necessary for optimal injector operation, providing support for both high impedance injectors and low impedance injectors.

- **Injection signal detection:** The module reliably detects ECU injection signals across various operating conditions, with appropriate signal conditioning to ensure consistent triggering thresholds.
- **Real-time pulse width manipulation:** Each individual injection pulse can be extended with precise timing control, allowing for dynamic fuel delivery adjustment.
- **Non-intrusive installation:** The module integrates between the ECU and the injector driver without requiring modifications to either component, preserving the integrity of the original system.
- **12V system compatibility:** All circuitry was designed to operate from standard 12V automotive electrical systems, with appropriate voltage regulation and protection.
- **Power management:** While the current implementation dissipates excess injector power as heat, this represents an area for potential future optimization.
- **Multi-cylinder support:** The modular design allows for expansion in order to drive multiple cylinders by stacking driver modules.
- **Parameter flexibility:** All parameters of the module can be configured and changed in real time, which makes tuning the system easier. A front-end interface for the module could be developed to make this process simpler.

## 7.3 Limitations and Challenges

Despite the successful implementation and tests, the conclusions to be drawn from this project are very limited, mostly due to the measurement limitations and the scope of the tests performed. The limited amount of data collected during the tests prevents further conclusions regarding the performance of the module.

The module was also only tested on a single motor, so the conclusions drawn from the tests are limited to the Weber motor used in this project. Conjectures can be made about the performance of the module on other motors, but these are not based on any practical tests.

Also the module itself has several limitations, the most important being:

- **Signal compatibility:** The current design is limited to detecting saturation-type injection pulses and cannot directly interface with peak and hold injection signals from more sophisticated ECUs.
- **Timing constraints:** The system can only extend injection events by delaying their termination, as there is no mechanism for predicting the start of subsequent pulses, limiting the control strategy options.
- **Injector capacity limits:** In alternative fuel applications, the stock injectors would likely become a performance bottleneck as their maximum duty cycle is constrained by engine speed. This would result in inadequate fuel delivery at higher loads, ultimately limiting power output without a corresponding injector system upgrade.
- **E-Fuel validation:** Although theoretically capable of supporting alternative fuels, practical testing with E-Fuels could not be completed due to the unavailability of suitable fuel samples and appropriate fuel system components.
- **Multi-cylinder validation:** While the design supports multiple cylinders and was validated with signal generators, practical testing was limited to a two-cylinder motor configuration.
- **Open-loop operation:** All testing was conducted on an engine without lambda feedback control, leaving closed-loop operation performance unverified.

## 7.4 Outlook

Future development of this technology should focus on addressing the identified limitations and expanding the system's capabilities:

- **E-Fuel testing:** The next logical step would be comprehensive testing with alternative fuels under controlled conditions with appropriate load simulation and data logging capabilities.

Analysis of combustion characteristics across various load conditions and extended operation would provide critical insights into long-term system viability.

- **Closed-loop control:** Implementation of lambda feedback control would significantly improve the precision of fuel mixture management, increasing flexibility and combustion quality.
- **Advanced control strategies:** Further development could explore predictive algorithms for injection timing, multiple injection events, and integration with additional engine parameters for more sophisticated fuel delivery control.
- **Hardware optimization:** Future iterations could improve power efficiency through regenerative techniques rather than dissipative current control, reducing thermal load and improving overall system efficiency.
- **Multi-cylinder testing:** Practical validation on engines with higher cylinder counts would confirm the scalability of the approach for more complex applications.

These advancements would address the current limitations while expanding the system's applicability to a wider range of alternative fuel conversion scenarios.

## References

- [1] Bundesumweltministeriums. *Häufig gestellte Fragen zu alternativen Kraftstoffen.* <https://www.bundesumweltministerium.de/WS5436>. (Visited on 28/07/2025).
- [2] Bundesumweltministeriums. *Was sind E-Fuels?* <https://www.bundesumweltministerium.de/FA1844>. (Visited on 28/07/2025).
- [3] Injector-Rehab. *Injector Drivers.* <https://injector-rehab.com/knowledge-base/injector-drivers/>. Image. (Visited on 30/07/2025).
- [4] André Kaufmann. 'Arbeitsheft Zu Verbrennungsmotoren'. Lecture Script.
- [5] Timm Kerscher. 'Faster Switching of Large Inductive Loads in Digital Output Modules'. Application Note. 2022.
- [6] Linear Products. 'Autmotive Fuel Injector Control Using Power+ Control with Power+ Arrays Devices'. Application Note. (Visited on 31/07/2025).
- [7] Monolithic Power Systems. *Fuel Injection and Ignition System Controls.* Image. URL: <https://www.monolithicpower.com> (visited on 30/07/2025).
- [8] Gordon P. Blair. *Design and Simulation of Four Stroke Engines.* SAE International, Aug. 1999. ISBN: 0-7680-0440-3.
- [9] Georges Saliba et al. 'Comparison of Gasoline Direct-Injection (GDI) and Port Fuel Injection (PFI) Vehicle Emissions: Emission Certification Standards, Cold-Start, Secondary Organic Aerosol Formation Potential, and Potential Climate Impacts'. In: *Environmental Science & Technology* 51.11 (June 2017), pp. 6542–6552. ISSN: 0013-936X. doi: 10.1021/acs.est.6b06509.
- [10] Kevin Shaw. *Weber MPE 850 Images.* <https://watercraftjournal.com/coming-soon-ski-near-weber-mpe-850-turbo-engine/>. Mar. 2014. (Visited on 02/08/2025).

- [11] H. Stančin et al. 'A Review on Alternative Fuels in Future Energy System'. In: *Renewable and Sustainable Energy Reviews* 128 (Aug. 2020), p. 109927. ISSN: 1364-0321. DOI: 10.1016/j.rser.2020.109927. URL: <https://www.sciencedirect.com/science/article/pii/S1364032120302185> (visited on 09/08/2025).
- [12] Texas Instruments. 'How to Drive Resistive, Inductive, Capacitive, and Lighting Loads'. Application Report. Feb. 2021. (Visited on 31/07/2025).
- [13] Texas Instruments. 'LM1949 Injector Drive Controller'. Datasheet. Feb. 1995. (Visited on 31/07/2025).
- [14] Textron Motors GmbH. 'INSTALLATION MANUAL 4-Stroke Engine MPE 850 MARINE'. Manual. Aug. 2013.
- [15] Zhi Tian et al. 'The Effect of Methanol Production and Application in Internal Combustion Engines on Emissions in the Context of Carbon Neutrality: A Review'. In: *Fuel* 320 (July 2022), p. 123902. ISSN: 0016-2361. DOI: 10.1016/j.fuel.2022.123902. (Visited on 29/07/2025).
- [16] Toshiba Electronic Devices & Storage Corporation. 'Parasitic Oscillation and Ringing of Power MOSFETs'. Application Note. URL: [https://toshiba.semicon-storage.com/info/application\\_note\\_en\\_20180726\\_AKX00066.pdf](https://toshiba.semicon-storage.com/info/application_note_en_20180726_AKX00066.pdf) (visited on 03/08/2025).
- [17] Krzysztof Więcławski, Jędrzej Mączak and Krzysztof Szczurowski. 'Electric Current Waveform of the Injector as a Source of Diagnostic Information'. In: *Sensors* 20 (July 2020), p. 4151. DOI: 10.3390/s20154151.

# **Attachment: Documentation of the Use of AI Tools**

In my scientific work/documentation, I have used AI tools as described below:

<b>Purpose of Use</b>	<b>AI Tool Used</b>	<b>Manner of Use</b>
LaTex Formatting and snippets	Claude 3.7	Used throughout the work
Spelling and grammar corrections	ChatGPT-4.1	Used on all written segments, throughout the writing process
Summarizing literature and other written sources	NotebookLM	Used throughout the work
Translations from German to English	DeepL	Translation of the statutory declaration